Norman Ruhnke (Autor)

A deep ultraviolet laser light source by frequency doubling of GaN based external cavity diode laser radiation

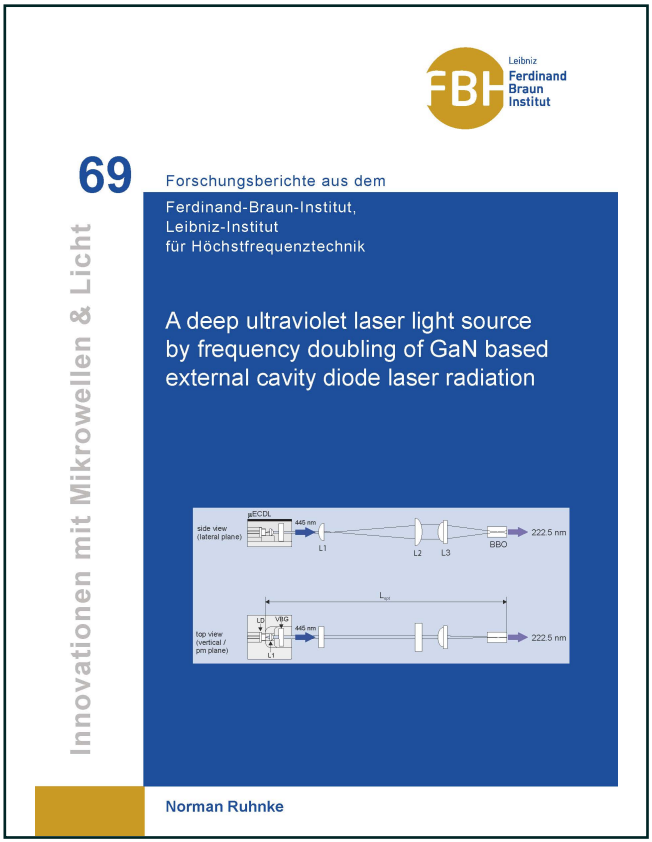

https://cuvillier.de/de/shop/publications/8642

1 Introduction

Motivation

The development of the laser diode with its high efficiency, compactness, robustness and long lifetime has enabled the construction of compact and non-sophisticated laser systems that have accessed many new applications outside of the laboratory environment. Nowadays, many fields of application such as information and communication technology, data storage, consumer electronics, materials processing, spectroscopy, biophotonics, and life science are addressed with laser diodes.

A spectral region, that is particularly interesting for numerous applications, is the wavelength range below 300 nm, hereinafter called deep ultraviolet (DUV). DUV light between 200 nm and 300 nm can sterilise bacteria, viruses and other pathogens by disrupting the structure of their DNA and can therefore be used for chemical-free disinfection of medical equipment [1–3], air conditioning systems and for water purification [4, 5].

It also has a great potential for sensing applications as many gases, that are major atmospheric pollutants and are primarily produced by fossil fuel combustion such as NO, NO_2, SO_2, and NH_3, exhibit strong electronic transitions in the wavelength region between 210 nm and 230 nm [6–8]. DUV absorption spectroscopy can be used to monitor the pollutant concentrations in ambient air. Typically, a spectral linewidth of about 5-10 cm^{-1} is usually sufficient for absorption spectroscopy of liquids and solids and in many cases also of gases [9].
Biomolecules and proteins such as tryptophan, NADH, tyrosine, DNA, RNA, and many others exhibit strong electronic transitions in the wavelength range below 250 nm as well and can be identified and quantified by DUV laser induced fluorescence (LIF) spectroscopy and related techniques [10–12]. In general, these techniques do not require a particularly narrow excitation linewidth and an excitation power of a few µW is sufficient [13].

Another prominent example for the wide range of application possibilities of DUV laser light is DUV Raman spectroscopy that can also be used for the identification of proteins and biomolecules [14, 15], explosives [16], and many other substances [17]. As the scattering cross section of the Raman signal scales with ω^4 and due to the possible excitation of resonant effects, the Raman signal can be enhanced by many orders of magnitude under DUV excitation compared to excitation with visible or NIR laser light [9]. Additionally, for excitation wavelengths below 260 nm, the Raman signal is spectrally separated from the usually much stronger and therefore disturbing fluorescence spectrum of most molecules [18]. Figure 1.1 further illustrates this situation with an exemplary Raman spectrum of the so-called fingerprint region of polystyrene exhibiting a spectral width of $\Delta\tilde{\nu} = 1600$ cm^{-1}. The hatched curve with the maximum at 600 nm represents a typical fluorescence background. For simplicity, all spectra are normalized to 1. Depending on the excitation wavelength λ_{ex}, the same Raman spectrum has a different spectral width on

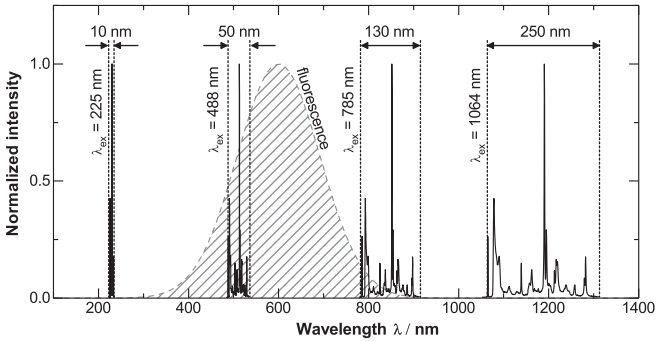

Figure 1.1: Illustration of the spectral separation of Raman signal and fluorescence background for DUV excitation using the example of the fingerprint region of the Raman spectrum of polystyrene.

the wavelength scale. For 225 nm excitation, it has a spectral width of only 10 nm and is spectrally separated from the fluorescence background. The spectral separation of Raman and fluorescence signal can also be used to obtain both signals in a single measurement which might be advantageous in some cases.

To resolve the investigated Raman spectra, the spectral emission bandwidth of the excitation laser light has to be in the range of the spectral width of individual Raman lines. For liquid and solid samples, these lines typically have a width of $\Delta\tilde{\nu} = 10\ \mathrm{cm}^{-1}$ [19]. For an excitation wavelength of $\lambda_{\mathrm{ex}} = 225$ nm, this translates into a required spectral width of $\Delta\lambda = 50$ pm on the wavelength scale.

Although higher optical output power is always desired, it was demonstrated that a DUV output power around 100 μW or even lower is already sufficient for absorption spectrocscopy of gases [20], for LIF detection [13], and DUV Raman spectroscopy [21, 22]. In a laboratory environment, an excitation power of a few nW was shown to be sufficient for absorption spectroscopy [7]. Especially when biological samples are under investigation too high output powers can lead to the destruction of the molecules as absorption in the DUV wavelength range is usually strong [22].

Table 1.1 summarizes the required wavelength range λ, average optical output power P_{opt}, and spectral linewidth $\Delta\tilde{\nu}$ in wavenumbers for a laser light source targeting these applications, which all have a great potential to be used outside of laboratory environments. This requires a compact and robust, if possible handheld and battery driven DUV laser light source. Within the frame of this work, the development and characterization of such a DUV light source based on laser diode emission is pursued that meets the physical requirements summarized in table 1.1 and utilizes the advantages of laser diodes in terms of robustness, small footprint and low power consumption.

Established DUV laser light sources Established laser light sources emitting in the DUV wavelength range are gas lasers and frequency-quadrupled solid state lasers. Table 1.2 gives an overview of the emission wavelength λ, average optical output power P_{opt}, and power consumption P_{con} of these laser systems.

Application	Technique	λ	P_{opt}	$\Delta\tilde{\nu}$
Sterilisation/disinfection of med. equipment and water purification	DNA disruption by absorption	200 - 300 nm	–	–
Gas/air analysis	Absorption spectroscopy	210 - 230 nm	$\geq$ nW	$< 10\ \text{cm}^{-1}$
Identification and quantification of proteins and biomolecules	Laser Induced Fluorescence (LIF) spectroscopy	210 - 230 nm	$\geq$ µW	–
	Raman spectroscopy	< 260 nm	$\geq$ µW	$\leq 10\ \text{cm}^{-1}$

Table 1.1: Possible applications for deep ultraviolet laser light, corresponding techniques, wavelength ranges, and required specifications.

Gas lasers like the KrF excimer laser (248 nm) [23] or the HeAg (224.3 nm) and NeCu (248.6 nm) hollow cathode lasers [24] directly emit in the wavelength range below 250 nm. The frequency doubled Ar^+ laser emitting at 244 nm [25, 26] is a well established DUV laser light source, too.
Despite offering high average output powers of more than 100 mW [23, 25, 26], KrF and Ar^+ lasers have a large footprint, a high power consumption of more than 1 kW [23, 25, 26], require frequent maintenance, and entail considerable production costs.
HeAg and NeCu hollow cathode lasers have a lower power consumption of less than 100 W, but deliver lower average output powers of less than 1 mW [24]. They also require frequent maintenance and have a relatively large footprint.
Another commonly applied solution is the generation of the fourth harmonic of Nd:YLF or Nd:YAG solid state lasers, that directly emit at infrared wavelengths of 1047 nm or 1064 nm, respectively. These systems deliver output powers of more than 10 mW, have smaller footprints and a moderate power consumption of around 100 W [27, 28]. Unfortunately, they only emit on fixed wavelengths of 262 nm or 266 nm, whereas an emission wavelength well below 250 nm is more suitable for the aforementioned applications.
DUV laser systems based on the generation of higher harmonics of the infrared emission from Ti:sapphire lasers offer tunable output in a wavelength range from 193 nm to 270 nm

Laser type	λ	mode	average P_{opt}	P_{con}
HeAg	224 nm	CW	< 1 mW	< 100 W
Ar^+ (2^{nd} harmonic)	244 nm	pulsed	> 100 mW	> 1 kW
KrF excimer	248 nm	pulsed	> 100 mW	> 1 kW
NeCu	249 nm	CW	< 1 mW	< 100 W
Nd:YLF (4^{th} harmonic)	262 nm	CW	> 10 mW	≈ 100 W
Nd:YAG (4^{th} harmonic)	266 nm	CW	> 10 mW	≈ 100 W
Ti:Sa (up to 4^{th} harmonic)	193 - 270 nm	pulsed	5 - 50 mW	> 1 kW

Table 1.2: Established DUV laser light sources and their emission wavelength λ, typical average optical output power P_{opt}, and power consumption P_{con}.

[29] together with excellent spectral and spatial beam properties. However, their high power consumption of more than 1 kW, their complexity and large footprint make them more suitable as scientific tools in the laboratory environment.

Each of the established light sources offers sufficient optical properties in terms of output power and emission linedwidth. However, they all have large footprints, high power consumptions and are rather complex, which usually restricts experiments to the laboratory environment. Furthermore, except for the Ti:sapphire based laser systems they all emit on fixed wavelengths only. To utilize DUV lasers in fields of application outside the laboratory environment as a portable *in situ* analysing and monitoring tool, a more compact and reliable DUV laser light source with minimal power consumption ideally suitable for battery operation is necessary. In this sense, a promising approach is frequency conversion of laser diode emission into the DUV wavelength range.

Diode laser based DUV light sources GaAs based laser diodes cover a wavelength range between 600 nm and 1200 nm with optical output powers in the watt range and reach wall-plug efficiencies of more than 70% [30] making them to the most efficient devices in converting electrical into optical energy [31]. Since the first demonstration of continuous wave emission from an InGaN based laser diode by Nakamura *et al.* in 1996 [32], also the green, blue, and parts of the ultraviolet spectral region can be addressed by direct emission from quantum well diode lasers. However, the shortest wavelength emitted by an electrically pumped AlGaN based laser diode so far is 336 nm [33] and direct DUV emission from laser diodes is still out of reach until now.

Therefore, a diode laser based DUV light source can only be realized by frequency conversion. A selection of relevant works on DUV frequency conversion of laser diode radiation is summarized in table 1.3. The concept of fourth harmonic generation of the infrared radiation of GaAs based laser diodes was already demonstrated in the 90s. It was realized by using either two successive single-pass (SP) [20, 34] or resonant cavity-enhanced (CE) [35, 36] frequency doubling (second harmonic generation, SHG) configurations. Goldberg [34] and Koplow [20] used very similar single-pass setups with a GaAlAs tapered amplifier (TA) laser diode emitting at 860 nm as pump source and a BBO crystal for DUV generation. Goldberg achieved a DUV optical output power of 15 µW at 215 nm. In the work of Kliner, the focus was on a minimized DUV emission bandwidth for absorption spectroscopy and an output power of 240 nW at 215 nm was generated.
Zimmermann *et al.* demonstrated a scheme with a GaAs master oscillator power amplifier (MOPA) laser diode (LD) emitting at 972 nm as pump source and two successive cavity-enhanced frequency doubling stages [35]. In the second stage, a BBO crystal was again used for the DUV generation of 2.1 mW at a wavelength of 243 nm. Schwedes *et al.* used a seeded GaAs tapered amplifier laser diode emitting at 922 nm to generate 1 mW of laser light at 231 nm [36] with a similar setup. The latter concept leads to higher DUV output powers than the single-pass arrangements, but can also become increasingly complex. A commercially available system from TOPTICA Photonics AG based on successive cavity-enhanced frequency doubling nowadays offers DUV output powers of 10 mW at 213 nm and even 300 mW at 266 nm [37, 42]. This system has a footprint of 9 cm x 41 cm x 69 cm and a power consumption of typically 100 W [42].

	Author	Laser type	Method	λ_{DUV}	P_{opt}
2x SHG	Goldberg (1995) [34]	GaAlAs TA	SP	215 nm	15 µW
	Koplow (1998) [20]	GaAlAs TA	SP	215 nm	240 nW
	Zimmermann (1995) [35]	GaAs MOPA	CE	243 nm	2.1 mW
	Schwedes (2003) [36]	GaAs TA	CE	231 nm	1 mW
	Toptica (2019) [37]	GaAs TA	CE	213 nm	10 mW
				266 nm	300 mW
SFG	Alnis (2000) [38]	GaN ECDL + GaAs LD	SP	254 nm	1 nW
	Carruthers (2005) [39]	GaN ECDL + GaAs LD	SP	254 nm	50 nW
	Anderson (2005) [40]	GaN ECDL + GaAs LD	SP	254 nm	4 nW
SHG	Nishimura (2003) [41]	GaN ECDL	CE	209 nm	9 µW

Table 1.3: Overview of diode laser based DUV light sources. SHG: second harmonic generation, SFG: sum frequency generation, TA: tapered amplifier, MOPA: master oscillator power amplifier, SP: single-pass, CE: cavity-enhanced.

Another approach is based on sum frequency generation (SFG) of the emission from a blue and a red emitting laser diode in a single-pass arrangement with BBO as nonlinear crystal [38–40]. In these works, only relatively low output powers in the nanowatt range were achieved and the concept has the inherent disadvantage of needing two laser diodes in operation.
A concept that leads to a DUV laser light source with further reduced footprint, power consumption, complexity, and overall production cost is direct second harmonic generation of GaN based laser diode radiation in the blue spectral range. This was already demonstrated by Nishimura *et al.* [41] using a low-power GaN external cavity diode laser (ECDL) as pump source. To achieve sufficient DUV optical output power, a BBO nonlinear crystal was integrated in an enhancement cavity. With this setup, a continuous wave (CW) output power of 9 μW at 209 nm was generated from 26 mW pump power at 418 nm. Besides this work, no further studies of this concept have been published so far.

Goal of this work

The goal of this work is to develop and characterize a novel diode laser based DUV light source with a smaller footprint and lower power consumption than previous light sources. The emission wavelength should be in the range between 210 nm and 230 nm with a continuous wave output power of about 100 µW and an emission bandwidth < 10 cm^{-1} or < 50 pm. Its specifications are defined by the applications referred to above and are listed in table 1.4.
The concept of direct second harmonic generation of GaN based laser diode radiation in the blue spectral range promises to result in the most compact and inexpensive DUV laser light source with minimal power consumption. Conversion efficiencies for DUV generation are quite low (typically 10^{-4} W^{-1}) usually making cavity-enhanced frequency doubling stages necessary [41]. However, with the recent development of commercially available

wavelength	λ	210-230 nm
output power	P	$\approx$ 100 µW
linewidth	$\Delta\tilde{\nu}$	$<$ 10 cm^{-1}
	$\Delta\lambda$	$<$ 50 pm
power consumption	P_{con}	$<$ 10 W

Table 1.4: Targeted specifications for the diode laser based DUV light source.

high-power GaN laser diodes emitting around 450 nm with output powers beyond 1 W [43, 44], direct single-pass frequency doubling of such laser diode radiation with DUV output powers around 100 μW has become feasible.
This work is intended to serve as proof-of-concept study, i.e. to demonstrate the feasibility of this concept and to investigate the physical challenges, that need to be considered.

The thesis is organized as follows: In chapter 2, the theoretical background that needs to be considered for DUV frequency doubling using a high-power GaN based laser diode, is presented. This includes fundamentals of nonlinear optics with an emphasis on second harmonic generation (SHG), an overview of crystals suitable for DUV generation, and estimations regarding the expected phase matching tolerances and nonlinear conversion efficiencies.
The applied laser diode (PL TB450B, OSRAM Opto Semiconductors) and its characteristics are presented in chapter 3. At the time of this work, the laser diode provided the highest optical output power of $P = 1.6$ W from a commercially available GaN based laser diode. Its broad spectral emission of $\Delta\lambda \approx 1...2$ nm full width at half maximum (FWHM) limits its applicability for efficient frequency conversion and does not meet the application requirements on the DUV light source listed in table 1.4. Hence, the emission bandwidth is reduced by implementing an external cavity diode laser (ECDL) setup. As this is a challenging and also crucial step for the development of the DUV light source, the concept is tested in a proof-of-principle ECDL system using surface diffraction gratings in Littrow configuration.
Chapter 4 starts with a brief description of wavelength stabilization of laser diodes by external optical feedback and a short literature review on GaN ECDLs with surface gratings. In section 4.2 and the following, the proof-of-principle ECDL system in Littrow configuration and its performance is analyzed. A miniaturized ECDL module (μECDL) with a volume Bragg grating as wavelength selective optical element is presented and discussed in section 4.3.
Both ECDL systems are demonstrated and evaluated in single-pass frequency doubling setups with BBO as nonlinear optical crystal in chapter 5. In section 5.1, the whole concept is again tested in a proof-of-principle setup by using the macroscopic ECDL in Littrow configuration as pump source. Here, challenges and difficulties of the single-pass concept regarding optimal focusing conditions and phase matching tolerances are discussed. The more compact DUV laser light source with the micro-integrated μECDL as pump source is presented in section 5.2 and the optimization of the focusing conditions is discussed in section 5.2.2.
Chapter 6 concludes this work, outlines different ideas on possible improvements of the compact DUV system and summarizes remaining challenges of the examined concept.

2 Fundamentals for frequency doubling with GaN based laser diodes

This chapter gives an overview of the relevant physical background for the realization of a DUV laser light source based on second harmonic generation (SHG) of blue GaN laser diode emission. A brief theoretical insight into nonlinear optics with a special emphasis on second order phenomena and second harmonic generation is given in section 2.1. The derivations of the necessary equations are thereby taken from the textbooks of William P. Risk *et al.* [45], Robert W. Boyd [46], and Richard L. Sutherland [47]. A full description of nonlinear phenomena can also be found in standard textbooks on nonlinear optics [46–48].

Section 2.2 gives an overview of nonlinear crystals suitable for frequency conversion into the ultraviolet wavelength range in general and discusses the advantages and disadvantages of different crystals with respect to second harmonic generation into the wavelength range below 250 nm. It will be shown that the nonlinear material of choice for the purpose of this work is β-BaB_2O (β-barium borate, BBO).
Using BBO for DUV generation by collinear second harmonic generation requires birefringent phase matching, which is explained in section 2.3. Here, the wavelength, temperature and angle tolerances for type I critical phase matching in BBO are calculated for the wavelength addressed in this work.
A brief summary of the Boyd-Kleinman theory that predicts the optimum focusing conditions inside the nonlinear crystal for circular Gaussian beams is given in section 2.4.

2.1 Nonlinear optics

The interaction of dielectric materials with the electric field $E(z,t)$ of an incident light wave propagating in z-direction is described by the polarization $P(z,t)$. For moderate intensities of the incident light, the response of the material is linearly dependent upon the strength of the electric field. However, for high intensities of the optical field as provided by lasers, the response of the material can be nonlinearly dependent upon the optical field strength. The first discovery of a nonlinear phenomenon was demonstrated by Franken et *al.* in 1961 [49]. They observed the second harmonic at a wavelength of 347 nm generated by irradiating a quartz crystal with a ruby laser emitting at a wavelength of 694 nm.

In nonlinear optics, the response of the material is usually generalized by expressing $P(z,t)$ as a power series in the field strength $E(z,t)$:

$$P(z,t) = \varepsilon_0 \left(\chi^{(1)} E(z,t) + \chi^{(2)} E^2(z,t) + \chi^{(3)} E^3(z,t) + ... \right), \tag{2.1}$$

where ε_0 is the vacuum permittivity, and $\chi^{(1)}$, $\chi^{(2)}$, and $\chi^{(3)}$ are the first, second, and third-order susceptibilities, respectively. The first term describes linear phenomena like the index of refraction. The second term with the square of the electric field leads to second order phenomena like second harmonic generation (SHG), sum frequency generation (SFG), difference frequency generation (DFG), parametric fluorescence or optical rectification. The third term with the cube of the electric field treats third order phenomena like third-harmonic generation, the intensity-dependent refractive index, or Brillouin scattering ([45], p. 23) .

For the description of SHG, only the second-order polarization $P^{(2)}(z,t)$ is considered in the following:

$$P^{(2)}(z,t) = \varepsilon_0 \chi^{(2)} E^2(z,t) \tag{2.2}$$

The strength of the induced polarization depends on the second-order susceptibility $\chi^{(2)}$ which is taken to be constant in equation (2.2). This assumption is justified, if all the frequencies taking part in the interaction are lying far below the lowest resonance frequency of the nonlinear material. For SHG, this condition is usually fulfilled and the nonlinear susceptibility is independent of the frequency ([46], p. 37).
In general, $\vec{P}(\vec{r},t)$ and $\vec{E}(\vec{r},t)$ are 3-dimensional vectors with components in x-, y-, and z-direction. The self-convolution of $\vec{E}(\vec{r},t)$ in equation (2.2) leads to 3 x 3 possible components for each of the three components of the second-order polarization. This means, that $\chi^{(2)}$ is actually a third-rank tensor written as $\chi^{(2)}_{ijk}$, where the indices i, j, k can independently take on the values x, y, and z leading to 27 different components [46]. Some symmetries fortunately reduce the number of independent components [46]. For instance, in the case of SHG, the indices j and k become interchangeable and can therefore be replaced by a new index l according to the following scheme ([46], p. 38):

jk	xx	yy	zz	yz,zy	xz,zx	xy,yx
l	1	2	3	4	5	6

The second-order susceptibility is then expressed by the contracted notation of the nonlinear

coefficient d_{il}, that is a 3 x 6 matrix with 18 components ([45], p. 28):

$$d_{il} = \frac{1}{2}\chi^{(2)}_{ijk} \tag{2.3}$$

Due to other symmetries including spatial crystal symmetries, the number of independent components in d_{il} is further reduced for most nonlinear crystals. A detailed discussion on the symmetries influencing the nonlinear susceptibility can be found in reference [46] (p. 32 *ff.*). The second-order polarization can now be re-written in the following form ([46], p. 38):

$$\begin{pmatrix} P^{(2)}_x \\ P^{(2)}_y \\ P^{(2)}_z \end{pmatrix} = 2\varepsilon_0 \underbrace{\begin{bmatrix} d_{11} & d_{12} & d_{13} & d_{14} & d_{15} & d_{16} \\ d_{21} & d_{22} & d_{23} & d_{24} & d_{25} & d_{26} \\ d_{31} & d_{32} & d_{33} & d_{34} & d_{35} & d_{36} \end{bmatrix}}_{d_{il}} \begin{pmatrix} E_x E_x \\ E_y E_y \\ E_z E_z \\ 2E_y E_z \\ 2E_x E_z \\ 2E_x E_y \end{pmatrix} \tag{2.4}$$

For known polarization and propagation directions of the participating waves, an effective nonlinear coefficient d_{eff} can be calculated and equation (2.2) can be expressed with scalar values (see [46], p. 39):

$$P^{(2)}(t) = 2\varepsilon_0 d_{\text{eff}} E^2(t) \tag{2.5}$$

2.1.1 Second harmonic generation

The electric field of a plane wave propagating in z-direction and oscillating with frequeny ω is written as:

$$E_1(z,t) = A_1 \cos(k_1 z - \omega t + \phi_1) \tag{2.6}$$

where A_1 is the amplitude of the electric field, k_1 is the wave vector, and ϕ_1 is the phase.

Inserting equation (2.6) into (2.5) gives the second-order polarization induced in a nonlinear material by the fundamental electric field $E_1(z,t)$:

$$P^{(2)}(z,t) = 2\varepsilon_0 d_{\text{eff}} \left[A_1 \cos(k_1 z - \omega t + \phi_1)\right]^2 \tag{2.7}$$

After using a simple trigonometric identity, an expression for the second-order polarization consisting of two terms is obtained:

$$P^{(2)}(z,t) = \varepsilon_0 d_{\text{eff}} A_1^2 \left[1 + \cos(2k_1 z - 2\omega t + 2\phi_1)\right] \tag{2.8}$$

The first term is at zero frequency giving rise to the process of optical rectification in which a static electric field is created within the nonlinear material. The second term in equation (2.8) oscillates at the second harmonic frequency 2ω. According to the inhomogeneous wave equation

$$\frac{\partial^2}{\partial z^2} E_2(z,t) - \frac{n_2^2}{c_0^2} \frac{\partial^2}{\partial t^2} E_2(z,t) = \frac{1}{\varepsilon_0 c_0^2} \frac{\partial^2}{\partial t^2} P^{(2)}(z,t), \tag{2.9}$$

the second-order polarization can be a source of a second electric field $E_2(z,t)$ oscillating with the frequency 2ω:

$$E_2(z,t) = A_2 \cos(k_2 z - 2\omega t + \phi_2) \tag{2.10}$$

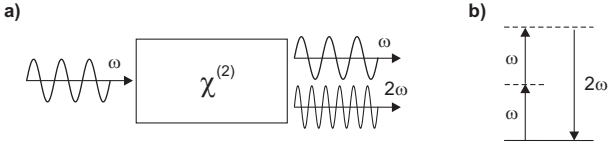

Figure 2.1: a) Schematic sketch of a second harmonic generation process inside a nonlinear crystal. b) SHG process depicted in an energy level diagram.

In this process, called second harmonic generation (SHG), two photons oscillating at frequency ω are transformed into one photon oscillating at the second harmonic frequency 2ω. Figure 2.1 illustrates the SHG process geometrically (a) and in an energy level diagram (b). By substituting equation (2.10) into (2.9) and applying the slowly varying amplitude approximation, one obtains a coupled-amplitude equation for the amplitude of the generated second harmonic wave (see [47], p. 57):

$$\frac{\mathrm{d}A_2}{\mathrm{dz}} = i\frac{2\omega d_{\mathrm{eff}}}{n_{2\omega}c}A_1^2 \cdot e^{i\Delta kz} \tag{2.11}$$

d_{eff} is the effective nonlinear coefficient, $n_{2\omega}$ the refractive index for the generated wave, and Δk is the wavevector mismatch:

$$\Delta k = 2k_1 - k_2. \tag{2.12}$$

The amplitude of the generated second harmonic wave can be derived by integrating equation (2.11) over the length L_{cr} of a nonlinear crystal:

$$\begin{aligned} A_2(L_{\mathrm{cr}}) &= i\frac{2\omega d_{\mathrm{eff}}}{n_{2\omega}c}A_1^2 \int_0^{L_{\mathrm{cr}}} e^{i\Delta kz}\,\mathrm{dz} \\ &= i\frac{2\omega d_{\mathrm{eff}}}{n_{2\omega}c}A_1^2 \left(\frac{e^{i\Delta kL_{\mathrm{cr}}}-1}{i\Delta k}\right) \end{aligned} \tag{2.13}$$

Substituting the amplitude for its intensity

$$I = 2\varepsilon_0 nc|A|^2, \tag{2.14}$$

gives with the use of (see [46], p.75)

$$\left|\frac{e^{i\Delta kL_{\mathrm{cr}}}-1}{\Delta k}\right|^2 = L_{\mathrm{cr}}^2\,\mathrm{sinc}^2(\Delta kL_{\mathrm{cr}}/2) \text{ and} \tag{2.15}$$

$$\text{and } \omega = 2\pi c/\lambda_\omega, \tag{2.16}$$

an expression for **the intensity of the generated second harmonic light**:

$$I_2 = \frac{8\pi^2 d_{\mathrm{eff}}^2}{\varepsilon_0 c n_{2\omega} n_\omega^2 \lambda_\omega^2} I_1^2 \cdot L_{\mathrm{cr}}^2 \cdot \mathrm{sinc}^2\left(\frac{\Delta kL_{\mathrm{cr}}}{2}\right) \tag{2.17}$$